Extending modified Cam-Clay to unsaturated soils by incorporating a scaled stress variable

Agostino Walter Bruno[1*], *Talenta* Pitso[1], *Leonardo Maria* Lalicata[1], *Adrian* De Paoli[2], and *Domenico* Gallipoli[1]

[1]Department of Civil, Chemical and Environmental Engineering, University of Genoa, 16145 Genoa, Italy
[2]Envirosoil (Remediation) Limited, SO32 2EJ Southampton, United Kingdom

Abstract. This paper extends the modified Cam-Clay model to describe the behaviour of unsaturated soils by replacing the effective stress with the scaled stress. The scaled stress accounts for the mechanical effect of capillarity by factoring Bishop's stress with a power function of degree of saturation. The extended modified Cam-Clay model postulates the existence of a yield curve in the mean scaled stress $\bar{p}$ – deviatoric scaled stress $\bar{q}$ plane. Coherently with the modified Cam-Clay model, the stress-strain behaviour is predicted by means of an elastic law inside the yield curve. As the scaled stress state evolves onto the yield curve, the behaviour becomes elasto-plastic and this is modelled by a plastic flow rule combined with a volumetric hardening law. The extended modified Cam-Clay model is then validated against experimental data published in the literature. Results show that the proposed approach is capable of well predicting the mechanical behaviour of unsaturated soils during triaxial loading. Future work will be directed at further validating the present formulation along different stress paths as well as accounting for the combined effect of partial saturation and cementation within a critical state framework based on bounding surface plasticity.

1 Introduction

The prediction of the mechanical behaviour of partially saturated soils relies on the definition of appropriate stress variables [1]. Initial studies have adopted a single effective stress approach [2-5] in an attempt to extend Terzaghi's principle [6] from saturated to unsaturated conditions. However, these single-stress formulations could not capture some features of the hydromechanical behaviour of partially saturated soils (e.g. wetting-induced collapse). Subsequent mechanical laws [e.g. 7-12] were formulated in terms of two independent stress variables, namely a tensorial stress variable (e.g. the net stress $\sigma_{ij} - \delta_{ij}u_a$, where σ_{ij} is the total stress, u_a is the pore air pressure δ_{ij} is the Kronecker delta) and a scalar stress variable (e.g. the matric suction $s = u_a - u_w$, where u_w is the pore water pressure). These two stress variables were combined with work-conjugate strain variables (e.g. the Cauchy mechanical strain and the water ratio hydraulic strain) to predict the behaviour of partially saturated soils [13]. The adoption of two independent stress variables surmounted some of the previous limitations at the cost, however, of an increased number of model parameters and greater analytical complexity. In an attempt to overcome such difficulties, this paper adopts the single scaled stress of Gallipoli and Bruno [14] to describe the behaviour of partially saturated soils under both isotropic and triaxial loading. The scaled stress accounts for the mechanical effect of capillarity by factoring the average skeleton stress, also known as the Bishop's stress, with a power function of the degree of saturation [14]. To demonstrate the ability of the proposed approach to capture the behaviour of unsaturated soils during triaxial loading, the modified Cam-Clay model [15] is recast in terms of scaled stresses instead of effective stresses. The resulting model is then calibrated and validated against experimental data by Raveendiraraj [16]. Predictions are compared with those of two other unsaturated soil models (i.e. Alonso et al. [7] and Wheeler et al. [8]) formulated in terms of two independent stress variables. Results show that the extended modified Cam-Clay model is capable of predicting the mechanical behaviour of partially saturated soils with similar accuracy of more complex two stresses formulations.

2 Extension of modified Cam-Clay to unsaturated soils

2.1 Constitutive variables

The scaled axial stress $\bar{\sigma}_a$ and scaled radial stress $\bar{\sigma}_r$ are respectively defined as the axial and radial Bishop's stresses, i.e. $\sigma'_a = \sigma_a - u_a + S_r(u_a - u_w)$ and $\sigma'_r = \sigma_r - u_a + S_r(u_a - u_w)$, scaled by a power function of degree of saturation, i.e. S_r^z, where the exponent z is a material parameter:

$$\bar{\sigma}_a = S_r^z \cdot [\sigma_a - u_a + S_r(u_a - u_w)] \quad (1)$$
$$\bar{\sigma}_r = S_r^z \cdot [\sigma_r - u_a + S_r(u_a - u_w)] \quad (2)$$

* Corresponding author: agostinowalter.bruno@unige.it

The exponent z controls the rate with which the scaled stresses tend to the Terzaghi's effective stresses as the degree of saturation tends to one. Moreover, the scaling factor S_r^z stems from the consideration that unsaturated soils can attain higher values of void ratio compared to saturated soils under the same stress levels, as described by Gallipoli and Bruno [14]. Equations (1-2) lead to the following expressions of the mean scaled stress $\bar{p}$ and deviatoric scaled stress $\bar{q}$:

$$\bar{p} = \frac{\bar{\sigma}_a + 2\bar{\sigma}_r}{3} = S_r^z \cdot [p - u_a + S_r(u_a - u_w)] \quad (3)$$

$$\bar{q} = (\bar{\sigma}_a - \bar{\sigma}_r) = S_r^z \cdot q \quad (4)$$

where p and q are the mean and deviatoric stresses, respectively. Note that the expression of mean scaled stress $\bar{p}$, given by Equation (3), is the product of two terms, namely the capillary bonding factor S_r^Z and the mean Bishop's stress $p' = p - u_a + S_r(u_a - u_w)$. These two terms may evolve in opposite directions during wetting at constant net stress as saturation increases while suction reduces. In this case, the mean scaled stress can either increase (inducing collapse compression) or decrease (inducing swelling) depending on which of these two terms dominates, as shown in Gallipoli and Bruno [14] and Bruno and Gallipoli [17].

The strain variables are the volumetric strain ε_v and the shear strain ε_s expressed as follows:

$$\varepsilon_v = \varepsilon_a + 2\varepsilon_r \quad (5)$$

$$\varepsilon_s = \frac{2}{3}(\varepsilon_a - \varepsilon_r) \quad (6)$$

where ε_a and ε_r are the axial and radial strain, respectively. In the modified Cam-Clay model [15], the increments of both the volumetric strain $d\varepsilon_v$ and shear strain $d\varepsilon_s$ are given by the sum of an elastic increment (i.e. $d\varepsilon_v^e$ or $d\varepsilon_s^e$) plus a plastic one (i.e. $d\varepsilon_v^p$ or $d\varepsilon_s^p$) as:

$$d\varepsilon_v = d\varepsilon_v^e + d\varepsilon_v^p \quad (7)$$

$$d\varepsilon_s = d\varepsilon_s^e + d\varepsilon_s^p \quad (8)$$

Similar to the modified Cam-Clay model [15], the present formulation also introduces a yield curve, an elastic law, a plastic potential and a volumetric hardening law, which are briefly recalled in the following section.

2.2 Extended modified Cam-Clay model

The extended modified Cam-Clay model postulates the existence of the following elliptical yield curve in the mean scaled stress $\bar{p}$ – deviatoric scaled stress $\bar{q}$ plane:

$$f = \bar{q}^2 - M^2\bar{p}(\bar{p}_0 - \bar{p}) = 0 \quad (9)$$

where M is a material parameter representing the slope of the critical state line in the mean scaled stress $\bar{p}$ – deviatoric scaled stress $\bar{q}$ plane, as given by the following relationship:

$$\bar{q} = M\bar{p} \quad (10)$$

Note that the slope of the critical state line in the mean scaled stress $\bar{p}$ – deviatoric scaled stress $\bar{q}$ plane, as defined by Equation (10), coincides with the slope of the critical state line in the mean Bishop's stress p' – deviatoric stress q plane, as both these stress variables are scaled of the same amount S_r^z.

In Equation (9), the preconsolidation mean scaled stress $\bar{p}_0$ is the hardening parameter controlling the size of the yield curve, i.e. the length of the major axis of the yield ellipse.

Upon virgin loading, the preconsolidation mean scaled stress $\bar{p}_0$ changes with the specific volume v according to the following semilogarithmic unified normal compression line:

$$v = N - \lambda \ln \bar{p}_0 \quad (11)$$

where λ is the slope of the unified normal compression line while N is the specific volume at a unitary mean scaled stress. The semilogarithmic unified normal compression line defined by Equation (11) is similar to the double logarithmic one of Gallipoli and Bruno [14]. A choice of a semilogarithmic relationship, instead of a double logarithmic one, has however been made here for consistency with the modified Cam-Clay [15].

The increment of volumetric strain $d\varepsilon_v$ can therefore be calculated from Equation (11) as follows:

$$d\varepsilon_v = -\frac{dv}{v_i} = \frac{\lambda d\bar{p}_0}{v_i\bar{p}_0} \quad (12)$$

where v_i and dv are respectively the initial value and the increment of specific volume. Overconsolidated soil states are described in the semilogarithmic plane of specific volume v – mean scaled stress $\bar{p}$ by unloading-reloading lines that start from the current preconsolidation values of specific volume v_o and mean scaled stress $\bar{p}_0$:

$$v = v_o - \kappa \ln\left(\frac{\bar{p}}{\bar{p}_o}\right) \quad (13)$$

where κ is the slope of the unloading-reloading lines. If the soil state moves along an unloading-reloading line inside the yield curve, the soil behaviour is reversible and the elastic increment of volumetric strain $d\varepsilon_v^e$ is calculated as:

$$d\varepsilon_v^e = -\frac{dv^e}{v_i} = \frac{\kappa d\bar{p}}{v_i\bar{p}} \quad (14)$$

The elastic increment of the shear strain $d\varepsilon_s^e$ is instead determined as:

$$d\varepsilon_s^e = \frac{d\bar{q}}{3G} \quad (15)$$

where G is the elastic shear modulus given by the following relationship:

$$G = \frac{3(1-2\nu)}{2(1+\nu)}\frac{v_i\bar{p}}{\kappa} \quad (16)$$

where ν is the Poisson ratio.

As the soil state reaches the yield curve and evolves onto it, the mechanical behaviour becomes elasto-plastic. The plastic volumetric strain increment $d\varepsilon_v^p$ is the difference between the total strain $d\varepsilon_v$ and elastic strain $d\varepsilon_v^e$ calculated by Equations (12) and (14):

$$d\varepsilon_v^p = d\varepsilon_v - d\varepsilon_v^e = \frac{(\lambda-\kappa)d\bar{p}_0}{v_i\bar{p}_0} \quad (17)$$

Equation (17) defines the volumetric hardening law of the model, which can be alternatively expressed as:

$$\frac{d\bar{p}_0}{d\varepsilon_v^p} = \frac{v_i\bar{p}_0}{\lambda-\kappa} \quad (18)$$

Assuming an associated flow rule with a plastic potential g equal to the yield curve f, the plastic increments of volumetric strain $d\varepsilon_v^p$ and shear strain $d\varepsilon_s^p$ are given as:

$$d\varepsilon_v^p = d\chi\frac{\partial g}{\partial\bar{p}} = d\chi M^2\bar{p}_0\left(\frac{M^2-\eta^2}{M^2+\eta^2}\right) \quad (19)$$

$$d\varepsilon_s^p = d\chi\frac{\partial g}{\partial\bar{q}} = d\chi M^2\bar{p}_0\left(\frac{2\eta}{M^2+\eta^2}\right) \quad (20)$$

where $d\chi$ is the plastic multiplier and η is the stress ratio between deviatoric scaled stress $\bar{q}$ and mean scaled stress $\bar{p}$. The combination of Equations (18) and (19) allows to recast the volumetric hardening law as:

$$d\bar{p}_0 = \frac{\partial\bar{p}_0}{\partial\varepsilon_v^p}d\varepsilon_v^p = \frac{v_i\bar{p}_0}{\lambda-\kappa}d\chi M^2\bar{p}_0\left(\frac{M^2-\eta^2}{M^2+\eta^2}\right) \quad (21)$$

By subsequently imposing the consistency condition:

$$df = \frac{\partial f}{\partial\bar{p}}d\bar{p} + \frac{\partial f}{\partial\bar{q}}d\bar{q} + \frac{\partial f}{\partial\bar{p}_0}d\bar{p}_0 = 0 \quad (22a)$$

or equivalently:

$$df = \frac{\partial f}{\partial\bar{p}}d\bar{p} + \frac{\partial f}{\partial\bar{q}}d\bar{q} + \frac{\partial f}{\partial\bar{p}_0}\frac{\partial\bar{p}_0}{\partial\varepsilon_v^p}d\varepsilon_v^p = 0 \quad (22b)$$

the following expression for the plastic multiplier $d\chi$ is obtained:

$$d\chi = \frac{\lambda-\kappa}{v_i\bar{p}M^2\bar{p}_0(M^2-\eta^2)}[(M^2-\eta^2)d\bar{p} + 2\eta d\bar{q}] \quad (23)$$

Finally, the plastic increments of volumetric strain $d\varepsilon_v^p$ and shear strain $d\varepsilon_s^p$ given by Equations (19-20) are recast as:

$$d\varepsilon_v^p = \frac{\lambda-\kappa}{v_i\bar{p}(M^2+\eta^2)}[(M^2-\eta^2)d\bar{p} + 2\eta d\bar{q}] \quad (24)$$

$$d\varepsilon_s^p = \frac{\lambda-\kappa}{v_i\bar{p}(M^2+\eta^2)}\left[2\eta d\bar{p} + \frac{4\eta^2}{M^2-\eta^2}d\bar{q}\right] \quad (25)$$

The above constitutive framework therefore requires calibration of six model parameters, i.e. the five parameters of the modified Cam-Clay model [15] N, λ, κ, ν, M plus the single parameter z accounting for partially saturated states. Calibration of parameter z requires tests on partially saturated soil samples with a minimum of one virgin isotropic loading at $s > 0\ kPa$. All other model parameters can be easily determined from conventional saturated tests. Both model calibration and validation are presented in the following sections.

3 Model calibration

The model parameters N, λ, κ, ν, M and z have been calibrated against the data set of Raveendiraraj [16] who tested a Speswhite kaolin soil with a liquid limit of 68% and a plastic limit of 34%, i.e. a plasticity index of 34%.

Soil samples were statically compacted to 400 kPa at a water content of 25%, resulting in a dry density of about 1200 kg/m^3. After compaction, the samples were subjected to a broad range of triaxial tests involving various types of stress paths, such as isotropic compressions at constant suction, wetting and drying at constant mean net stress and shearing at constant radial stress and suction.

Part of these experimental data was used to calibrate the parameters of the extended modified Cam-Clay model. In the absence of a soil-water retention law (e.g. [18]), experimental instead of predicted values of degree of saturation were substituted inside the scaled stress expressions of Equations (3-4). This is, however, preferable during calibration and validation of the proposed mechanical model to avoid that the predicted behaviour may be influenced by the level of accuracy of the chosen retention law.

Figure 1 shows the calibration of the parameters N, λ and z against isotropic loading paths at constant suctions of 0 (i.e. fully saturated conditions), 50, 150 and 350 kPa. Inspection of Figure 1 indicates that, both unsaturated and saturated virgin soil states are well described by the unified isotropic normal compression line of Equation (11) expressed in terms of mean scaled stress. This is, however, an expected results as the normalising effect of the scaled stress variable and the regularisation of saturated and unsaturated behaviour onto a unique isotropic virgin line have already been extensively demonstrated by Gallipoli and Bruno [14] and Bruno and Gallipoli [17] for a broad variety of soils, ranging from both kaolin and bentonite clays to loess silts.

The model parameter κ was instead calibrated against an isotropic unloading path from a mean net stress of 150 kPa to 75 kPa at a constant suction of 150 kPa, as shown in Figure 2. The Poisson ratio was taken equal to 0.33 as indicated by Black et al. [19], who tested similar Speswhite kaolin samples as Raveendiraraj [16].

Finally, the model parameter M was calibrated against critical state data plotted in the mean scaled stress $\bar{p}$ – deviatoric scaled stress $\bar{q}$ plane, as shown in Figure 3. Note that the resulting value of the parameter M is equal to that determined by Raveendiraraj [16] during calibration of the model by Wheeler et al. [8], whose stress variables are the mean Bishop's stress p' and the deviatoric stress q. As already mentioned, this is because the critical state line is identical for both sets of stress variables.

Table 1 summarises the values of all calibrated parameters, which have then been used for the validation of the extended modified Cam-Clay model as described in the following section.

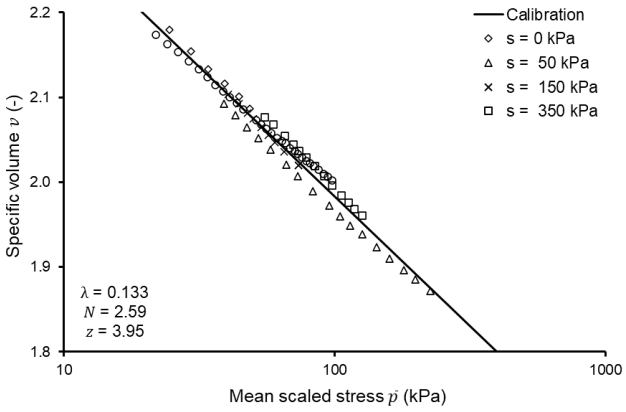

Fig. 1. Fitting of the unified isotropic normal compression line to experimental data by Raveendiraraj [16].

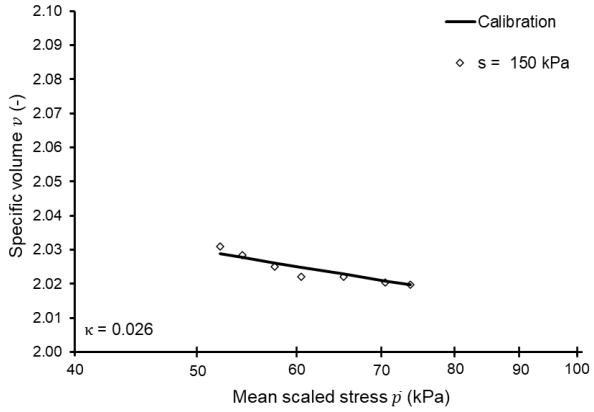

Fig. 2. Fitting of an unloading-reloading line to experimental data by Raveendiraraj [16].

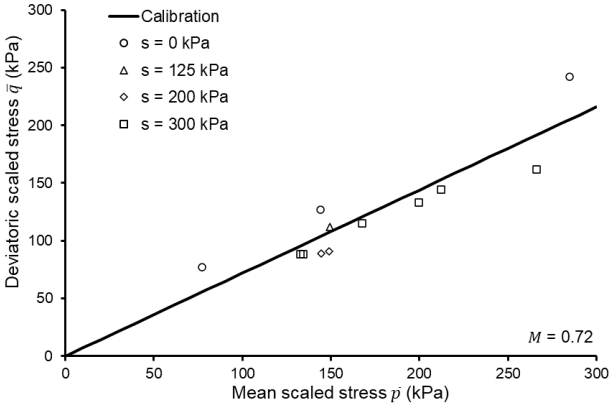

Fig. 3. Fitting of the critical state line to experimental data by Raveendiraraj [16].

Table 1. Calibration of model parameters against experimental data by Raveendiraraj [16].

Model parameters	
λ (-)	0.133
N (-)	2.59
z (-)	3.95
κ (-)	0.026
ν (-)	0.33
M (-)	0.72

4 Model validation

Model predictions have been validated against experimental data not considered during calibration (i.e. blind prediction). Only triaxial paths performed by increasing the axial stress while maintaining constant both radial stress and suction have been considered as the viability of the scaled stress under isotropic paths has already been extensively validated by Gallipoli and Bruno [14] and Bruno and Gallipoli [17].

Experimental rather than calculated values of degree of saturation were used for calculating the scaled stress variables, which is preferable as previously discussed. Nevertheless, for practical applications, a suitable retention law will need to be coupled with the present formulation to calculate the degree of saturation during a generic stress/suction path. The coupling of the proposed mechanical law with a soil-water retention law, similar to [18], is matter for future research.

Figures 4 and 5 show the experimental data from two shearing stages performed at the constant radial net stress of 75 kPa and at the two constant suctions of 200 kPa and 300 kPa, respectively. Experimental data are shown together with the corresponding model predictions in terms of deviatoric stress q – shear strain ε_s (Figures 4a and 5a) and volumetric strain ε_v – shear strain ε_s (Figures 4b and 5b). The predictions from the constitutive laws of Alonso et al. [7] and Wheeler et al. [8], as calculated by Raveendiraraj [16], are also reported.

Figures 4 and 5 also include model predictions by considering a non-associated flow rule that scales the plastic shear strain increment $d\varepsilon_s^p$ by a factor α as:

$$d\varepsilon_s^p = \frac{\alpha(\lambda-\kappa)}{v_i\bar{p}(M^2+\eta^2)}\left[2\eta d\bar{p} + \frac{4\eta^2}{M^2-\eta^2}d\bar{q}\right] \quad (26)$$

In Equation (26), the value of the factor α is chosen to predict zero lateral strain during K_0 loading paths according to Jaky [20], i.e. $K_0 = 1 - \sin\varphi' = (6 - 2M)/(6 + M)$. This assumption, firstly introduced by Ohmaki [21] and subsequently adopted by Alonso et al. [7], is particularly convenient because it allows to express the factor α in terms of previously defined model parameters as:

$$\alpha = \frac{M(M-6)(M-3)}{9(6-M)}\left[\frac{1}{1-\frac{\kappa}{\lambda}}\right] \quad (27)$$

A value of $\alpha = 0.37$ is calculated from Equation (27) corresponding to the values of parameters λ, κ and M indicated in Table 1.

Inspection of both Figures 4a and 5a indicates that the extended modified Cam-Clay model underestimates the deviatoric stress at any given shear strain. This discrepancy is however mostly attributable to the associated flow rule of the original model rather than to the single scaled stress approach. Predictions are much improved by the introduction of the non-associated flow rule, leading to a level of accuracy similar to that of the models of Alonso et al. [7] and Wheeler et al. [8], formulated in terms of two independent stress variables.

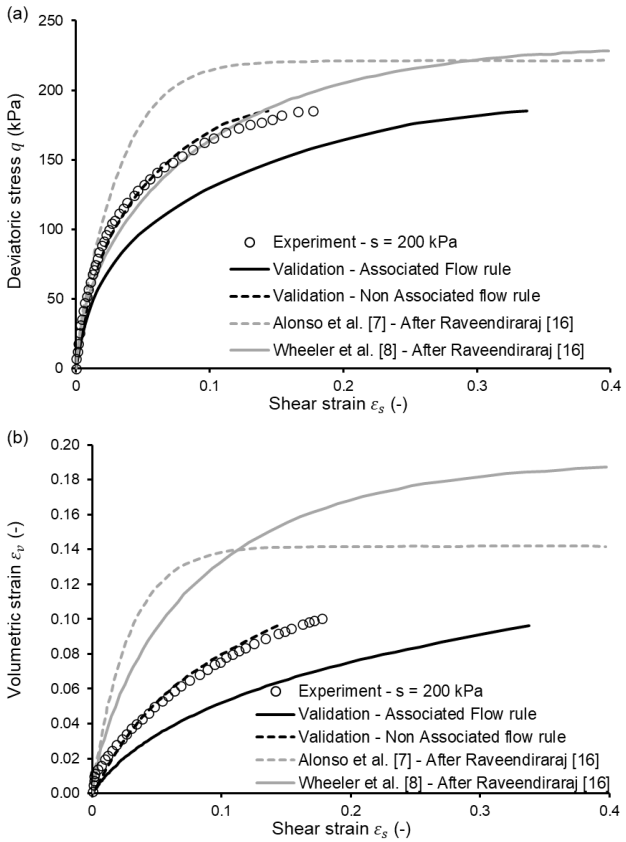

Fig. 4. Model prediction against shearing at a constant suction of 200 kPa taken from Raveendiraraj [16].

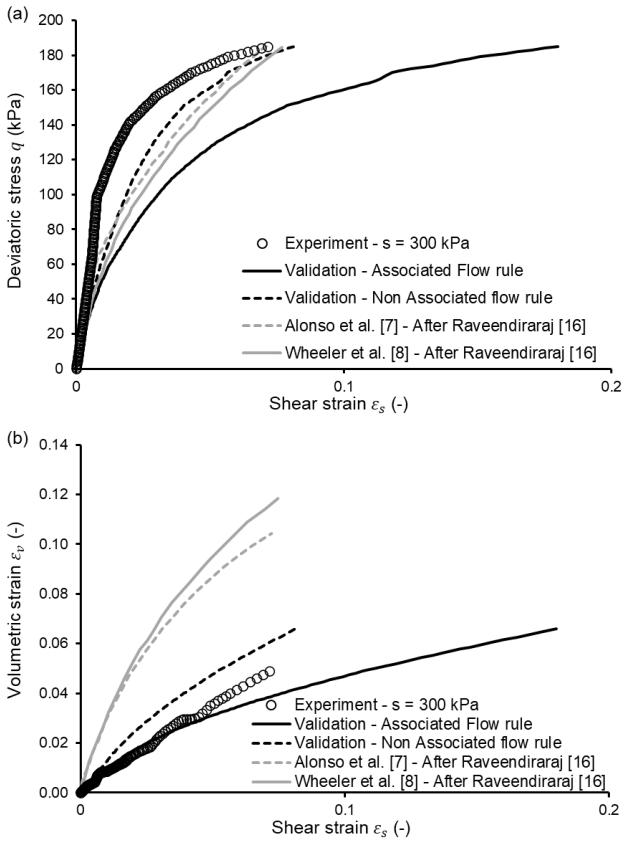

Fig. 5. Model prediction against shearing at a constant suction of 300 kPa taken from Raveendiraraj [16].

Inspection of Figures 4b and 5b shows that the extended modified Cam-Clay model well predicts the volumetric behaviour of the soil during shearing. The quality of the computed results improves when the non-associated flow rule is introduced leading to even better predictions than those from Alonso et al. [7] and Wheeler et al. [8]. Note, however, that the experimental results considered in the present work are limited to 'wet and loose' soil samples that exhibit a strain-hardening behaviour under shearing. Future work will need to extend the present study to the prediction of the unsaturated strain-softening behaviour of 'dry and dense' soils.

The above preliminary results suggest that a single scaled stress modelling approach may be viable for reproducing the behaviour of partially saturated soils. They also indicate that the choice of a different associated plasticity model from modified Cam-Clay [15] (e.g. a model incorporating kinematic and volumetric hardening with a rotated yield ellipse) may improve predictions. This aspect is, however, outside the scope of the present work and future research will be developed in this direction.

5 Conclusions

This paper has presented an extension of the modified Cam Clay model [15] to predict the mechanical behaviour of partially saturated soils by replacing the effective stress of the original formulation with the scaled stress of Gallipoli and Bruno [14]. The scaled stress is defined as the product of Bishop's stress and a power function of the degree of saturation. The proposed framework therefore includes the five parameters of the modified Cam-Clay [15], which can be determined via conventional saturated tests, plus one parameter of the scaled stress of Gallipoli and Bruno [14], which must be determined via unsaturated testing.

Similar to modified Cam Clay [15], the present approach postulates the existence of a yield curve in the mean scaled stress $\bar{p}$ – deviatoric scaled stress $\bar{q}$ plane inside which the soil behaviour is elastic. As the soil state reaches the yield curve and evolves onto it, the soil behaviour becomes elasto-plastic and strain increments are determined by means of an associated flow rule combined with a volumetric hardening law. Additional predictions have also been produced by introducing the non-associated flow rule proposed by Ohmaki [21]. This non-associated flow rule scales the plastic shear strain increment by a factor α, whose value is determined by imposing zero lateral strain under K_0 loading.

The extended modified Cam-Clay model has been calibrated and validated against experimental data by Raveendiraraj [16], who tested Speswhite kaolin samples under both saturated and unsaturated triaxial paths. Results show that the proposed model well captures the experimental values of deviatoric stress, shear strain and volumetric deformation. Interestingly, the quality of the prediction is comparable to that of more sophisticated mechanical laws expressed in terms of two independent stress variables. The calculated stress-stain response becomes even more accurate when

the non-associated flow rule is introduced suggesting that part of the discrepancies observed in the present study may be attributable to shortcomings of the reference saturated model.

Future work will aim at further validating the proposed modelling approach against different stress paths and accounting for the simultaneous effect of partial saturation and cementation similar to [22-23]. These developments may also incorporate a more realistic critical state framework based on bounding surface plasticity.

References

1. D. Gallipoli, P. Grassl, S. Wheeler, A. Gens, Geomech. Energy Environ. **15**, 3-9 (2018)
2. G. D. Aitchison, I. B. Donald, In Proceedings 2nd Australia-New Zealand Conference on Soil Mechanics and Foundation Engineering, Christchurch, 192-199 (1956)
3. A. W. Bishop, I. B. Donald, In Proceedings 5th International Conference on Soil Mechanics and Foundation Engineering, 13-21 (1961)
4. A. W. Bishop, G. E. Blight, Geotechnique **13**, 3, 177-197 (1963)
5. J. B. Burland, In Moisture equilibria and moisture changes beneath covered areas, Sydney: Butterworths, 270-278 (1965)
6. K. Terzaghi, In Proceedings 1st International Conference in Soil Mechanics 1, 54-56, (1936)
7. E. E. Alonso, A. Gens, A. Josa, Geotechnique **40**, 3, 405-460 (1990)
8. S. J. Wheeler, R. S. Sharma, M. S. R. Buisson Geotechnique **53**, 1, 41-54 (2003)
9. D. Mašín, N. Khalili, Int J Numer Anal Methods Geomech, **32**, 15, 1903-1926 (2008)
10. L. Laloui, M. Nuth, Comput Geotech, **36**, 1-2, 20-23 (2009)
11. R. Hu, H. H. Liu, Y. Chen, C. Zhou, D. Gallipoli, Comput Geotech, **59**, 127-144 (2014)
12. M. Lloret-Cabot, S. J. Wheeler, M. Sánchez, Acta Geotech., **12**, 1-21 (2017)
13. J. Vaunat, E. Romero, C. Jommi, In Experimental Evidence and Theoretical Approaches in Unsaturated Soils, Rotterdam: Balkema, 121–138 (2000)
14. D. Gallipoli, A. W. Bruno, Geotechnique **67**, 8, 703-712 (2017)
15. K. Roscoe, J. B. Burland, in Engineering Plasticity, Cambridge, 535-609 (1968)
16. A. Raveendiraraj, PhD thesis, University of Glasgow, Glasgow, UK (2009)
17. A. W. Bruno, D. Gallipoli, Comput Geotech, **110**, 287-295 (2019)
18. D. Gallipoli, A. W. Bruno, F. D'Onza, C. Mancuso, Geotechnique **65**, 10, 793-804 (2015)
19. J. A. Black, V. Sivakumar, A. Bell, Geotechnique **61**, 11, 909-922 (2011)
20. J. Jaky, In Proceedings 2nd International Conference on Soil Mechanics and Foundation Engineering **1**, 103-107 (1948)
21. S. Ohmaki, In Numerical models in geomechanics. International Symposium, Zurich: Balkema, 260–269 (1982)
22. A. W. Bruno, D. Gallipoli, M. Rouainia, M. Lloret-Cabot, Comput Geotech, 125, 103673 (2020)
23. A. W. Bruno, D. Gallipoli, M. Rouainia, M. Lloret-Cabot, In Proceedings 4th European Conference on Unsaturated Soils (2020), 195, 02001.